Journal of Bio- and Tribo-Corrosion (2022) 8:71
https://doi.org/10.1007/s40735-022-00669-x

Mechanism of Corrosion and Microbial Corrosion of 1,3-Dibutyl Thiourea Using the Quantum Chemical Calculations

Elshafie A. Gad[1] · **Ashraf M. El-Shamy**[2]

Received: 11 February 2022 / Revised: 21 April 2022 / Accepted: 10 May 2022 / Published online: 27 May 2022

Abstract
An investigation of the inhibiting behavior of 1,3-dibutyl thiourea (DBTU) against corrosion and microbiological corrosion on carbon steels in highly salted (3.5% w/w NaCl) environments at ambient temperature and pressure was undertaken. That it works well at low doses for both corrosion and microbiological corrosion was established. The findings of the study show that DBTU inhibits corrosion well and in terms of microbial corrosion, it had a little impact on planktonic bacteria and a minor effect on sessile bacteria. On this compound's damping effect, we used OCP, PD, and EIS. Afterward, the surface was characterized using quantum chemical computations. This study identified the optimal dose of 50 ppm. The findings indicated that inhibitor adsorption is the main source of inhibition procedure. The findings reveal that the inhibitor's thin layer protected the carbon steel surface in highly corrosive salt conditions. An average of 95.36% of DBTU was found to have an inhibitory effect at a concentration of 50 parts per million. The connection between DBTU and the carbon steel surface was very strong and remained strong throughout a broad range of temperatures.

Keywords Corrosion inhibition · 1,3-Dibutyl thiourea · Oil field industry · Microbial corrosion

1 Introduction

For many decades, DBTU has been studied as a steel corrosion regulator, functional density theory, and laboratory DBTU research and its variants [1, 2]. The effect of DBTU addition on the degradation of 70 Cu–30 Ni alloys and carbon steels in NaCl solutions has been documented at pH 18–20 in liquid water and surface water [3–5]. At 60 °C, the effect of DBTU load on the corrosion of the two alloys has been measured in both mediums. The use of inhibitors has been proven to be an effective and widely accepted approach to corrosion prevention. This page discusses the many corrosion-fighting chemicals present in acid water. Several examples of heat-combatant agents found in acidic media are given in the article [6–8]. Research highlights the avoidance of acid media weathering in steel materials. Acidic solutions have several anti-corrosion properties for steel constructions. The arrangement of a part in an aqueous solution with low molecular polarity promotes the synthesis of a corrosion inhibitor [9–11].

Surface analyses suggested that CA molecules may be released from the assembly in a parallel way, accompanied by energy rivalry and adsorption exclusively on the steel's surface, as supported by theoretical modeling [12–14]. Such a consideration might be beneficial in the development of new DBTU compounds, such as steel corrosion inhibitors. DBTU in various poor media has also been shown to have a remarkable inhibitory effect on steel in experiments and according to DFT simulations. For many decades, DBTU and its variants have been evaluated for corrosion resistance with steel. Because the mechanisms of interaction with metallic structures are unknown, it may be required to develop novel DBTU compounds for use as corrosion inhibitors in steel structures [15–17].

The combination of ethanol and SLES significantly increases inhibitory efficacy and creates a strong synergistic effect [18]. Metal surfaces are protected by accumulating layers of organic matter to make the corrosive inhibition process highly effective, and to ensure this, the various defenses are analyzed and compared with the electrochemical kinetic

✉ Ashraf M. El-Shamy
elshamy10@yahoo.com; am.elshamy@nrc.sci.eg

[1] Egyptian Petroleum Research Institute, 1 Ahmed El-Zomor Street-El-Zohour Region Nasr city, Cairo 11727, Egypt

[2] Electrochemistry and Corrosion Lab., Physical Chemistry Department, National Research Centre, El-Bohouth St. 33, Dokki, P.O. 12622, Giza, Egypt

properties, as well as the morphological and chemical properties resulting from organic matter adsorption on mineral surfaces. As a result, under the identical test circumstances used in this article, sodium citrate was demonstrated to be more effective in preventing corrosion. The layer accumulation and formation process of single or multiple layers of DBTU on the metal surface, particularly self-assembled monolayers of octa decanethiol, was also investigated using an electrochemical tool, a periodic potentiometer, and an alternating current resistance spectroscopy system [19–21].

The notion of utilizing dextran in a high acid environment as a safe defender for steel was examined using PDP experiments, where dextran worked as a varied form corrosion inhibitor. The dextran inhibition effectiveness changes inversely with molar mass but particularly with temperature [22]. A deformation is a natural occurrence, yet it is controllable. Aside from the toxicity issues of composites such as chromium-based inhibitors, the creation, and usage of eco-friendly inhibitors, often known as green inhibitors, is a growing source of concern. This research quickly examines some of the intriguing properties observed by green inhibitors during the previous decade [23].

The purpose of this research is to investigate the efficiency of corrosive inhibition of DBTU, particularly on immersed carbon steel in 3.5% w/w sodium chloride, using electrochemical techniques to examine it and the effect of concentration rates to achieve the best concentration and best results under these pressure and temperature conditions, and then study this concentration in inhibiting microbial corrosion of the two types of bacteria suspended in the solution [24–26].

2 Material and Methods

All the materials utilized in this investigation are commercially available springs. These materials were purchased with a high purity of the analytical grade, and care was made to verify that they were free of impurities to assure the correctness of the findings. As a result, Sigma-Aldrich was used to get high purity sodium chloride, methanol, ethanol, and DBTU. The inhibitor DBTU was treated scientifically to guarantee the best results were obtained by undergoing a dissolving procedure with less than 1% methanol and a 3.5% w/w NaCl solution. Carbon steel samples were subjected to elemental analysis to determine the omitted various components in the samples under examination. It was discovered that the average proportions of the various components. The remaining components were 0.097% C, 0.49% Mn, 0.020% P, 0.09% Si, 0.05% Cr, 0.11% Ni, 0.16% Cu, 0.042% S, and Fe. The samples were created to meet the specifications of the experiment [27].

2.1 Optimization of Inhibitors Loading

The weight loss technique is one of the ways used to assess this stabilizer. Glass containers having a capacity of 100 mL from a Pyrex container were used for these tests. Experiments were carried out with and without DBTU. To produce various concentrations of DBTU, these specific concentrations were prepared from the whole solution by liquifying one gram of the inhibitor in 100 mL of distilled water as a single solution to carry out the entire research from one solution for all tasks [28].

2.2 Measurements of Potentiodynamic Polarization

Electrochemical techniques were utilized to perform the inhibitor's corrosive assessments, which was one of the ways used to evaluate this inhibitor. These tests were carried out with the help of a Potentiostat/Galvanostat (PGSTAT302N) that was tested with Auto lab (NOVA) software, allowing for effective dynamic scanning of coupons via the use of an electrochemical cell, which traditionally consists of three electrodes, to form an encapsulated corrosion cell. The reference electrode was silver/silver chloride (Ag/AgCl), the counter electrode was platinum, the working electrode was carbon steel, and the conduction was done in series. It should be noted that the materials used in the construction of the working electrode are the same as those used in all other measurements [29, 30].

2.3 Surface Characterization

The coupons under study were imaged using a scanning electron microscope equipped with a Philips-30 emission field and an Oxford device to detect energy dispersive X-rays in the secondary, scattered, and backlash modes of the electron with a 15 kV acceleration voltage to evaluate and understand the mechanism of the effect. Surface morphology was used under these conditions to detect the existing elements on the metallic surface using FESEM/EDX methods [31, 32].

2.4 Microbial Corrosion Measurements

2.4.1 Planktonic Bacteria

Collect field water samples as directed by NACE TM0194. Begin testing immediately after the sample has been obtained. Make the testing conditions as like those encountered in the system as possible. For anaerobic systems, for example, testing should be done in nitrogen- or argon-purged bottles that are commercially available. The bacteria used to evaluate the biocides should be representative of

the population found in the test fluid. In addition, up to 1% inoculum of a fully grown culture from the field system may be used. To prevent adding superfluous organic material to the test systems, utilize no more than 1% inoculum. Biocides can be diluted to 1 to 10% of the initial product in sterile bottles (30 to 200 mL) for more accurate dosing. The amount of stock solution added to each bottle (test system) should be calculated to produce one of the dose rates expected to be helpful in the system (once the bottle is filled with field water) [33].

The biocide dose range should be found on the label. Fill six bottles with distilled water instead of a biocide stock solution to act as controls for the field water. Biocides can be diluted to 1 to 10% of the initial product in sterile bottles (30 to 200 mL) for more accurate dosing. The amount of stock solution added to each bottle (test system) should be calculated to produce one of the dose rates expected to be helpful in the system (once the bottle is filled with field water). The biocide dose range should be found on the label. Fill six bottles with distilled water instead of a biocide stock solution to act as controls for the field water. Fill the test bottles with the test fluid, both those containing the biocide dilutions and those containing the control bottles (containing bacteria). To determine the number of live bacteria that were initially present in the test bottles, thoroughly mix them and promptly remove 1 mL samples from the control bottles [34].

To prevent oxygen from entering test systems, septum seals should be used. Select biocide exposure periods (test system holding times) that match biocide contact times in the field system. After these times, collect 1 mL samples from each dilution of each biocide being evaluated, as well as the controls, to determine the viable bacterial population. This testing is most reliable when the test procedure closely resembles the field system's normal operating circumstances, including the presence of average quantities of production chemicals; hence, the user must modify the technique to meet a given system. False results may arise in the first or second serial dilutions with the higher biocide dosages used due to the transfer of significant biocide concentrations (which function as a biostatic) from the test fluid to the growth medium. These tests are only for planktonic species. This method cannot assess the efficacy of biocides in suppressing sessile bacteria in the system. Biocides are frequently less effective against sessile bacteria than against planktonic bacteria [35].

2.4.2 Sessile Bacteria

Coupons containing biofilm can be used to assess the effectiveness of biocide treatments against sessile bacteria. Coupon-based biofilm samples should be removed before, during, and after biocide treatment. Surviving bacteria should be examined in the same manner as stated above.

Biocides should be applied to sessile bacteria on coupons under static conditions or in dynamic flow loops for time-kill testing. Because biofilm development is so essential, different test procedures for assessing biocide efficacy can be used, including stagnant bottle tests, re-circulating loops, and once-through systems (i.e., dynamic flow cells). Although this testing is not addressed by this standard, there is published information on these testing procedures available. Electrochemical probes and biosensors are two types of probes that may be used to assess the efficacy of biocides [36].

3 Results

3.1 Electrochemical Techniques

The findings shown in Fig. 1A demonstrated the degree of the growth of the rate of degradation in corrosion rates and a clear rise in the inhibition efficiency when the damper doses were changed in the ambient temperature, pressure, and air conditions. The corrosion risk should be minimized to at least 0.0504 mg cm^2 hour with an initial dosage of 0.05 g/L (or 50 ppm) of DBTU. The same region of inhibitor dosages demonstrated significant increases in receptor effectiveness, surpassing 95.36%. A relatively modest dosage of DBTU (0.05 g/L or 50 ppm) has been shown to have a 40% inhibitory effectiveness. Previous research revealed that the results correspond well with the previously described research [37]. Carbon steel tests were carried out using one of the electrochemical approaches, the polarization model, which yielded curves displaying the cellular carbon steel. At the pressure and temperature parameters depicted in Fig. 1B. Corrosion dynamics are depicted in this figure. The Tafel polarization may be inferred from the provided data (Table 1).

Whereas the cathodic branch represents the medium's interaction with the samples, the carbon nitric nit, through which hydrogen evolution and escalation appears under the specific conditions of the experiment, the anodic branch explains the reaction of steel dissolution, which explains the phenomenon of corrosion. It also emerges from the Tafel lines that are used to estimate the fixed erosive potential as seen in Fig. 1B. As demonstrated in Fig. 1B, almost all the existing anodic and cathodic densities decreased, suggesting that DBTU facilitated anodic and cathodic interactions via adsorption on the metallic surface. As this DBTU combination has dual effects (anode and cathode), it is resistant to the corrosive action of a 3.5% NaCl solution [38].

EIS may examine diverse relaxation processes in non-destructive locations and procedures with a broad frequency spectrum [39]. The provided Nyquist and Bode electrode diagrams of the corrosive behavior of carbon steel in saline environments [40] are shown in Fig. 1C. The capacitance

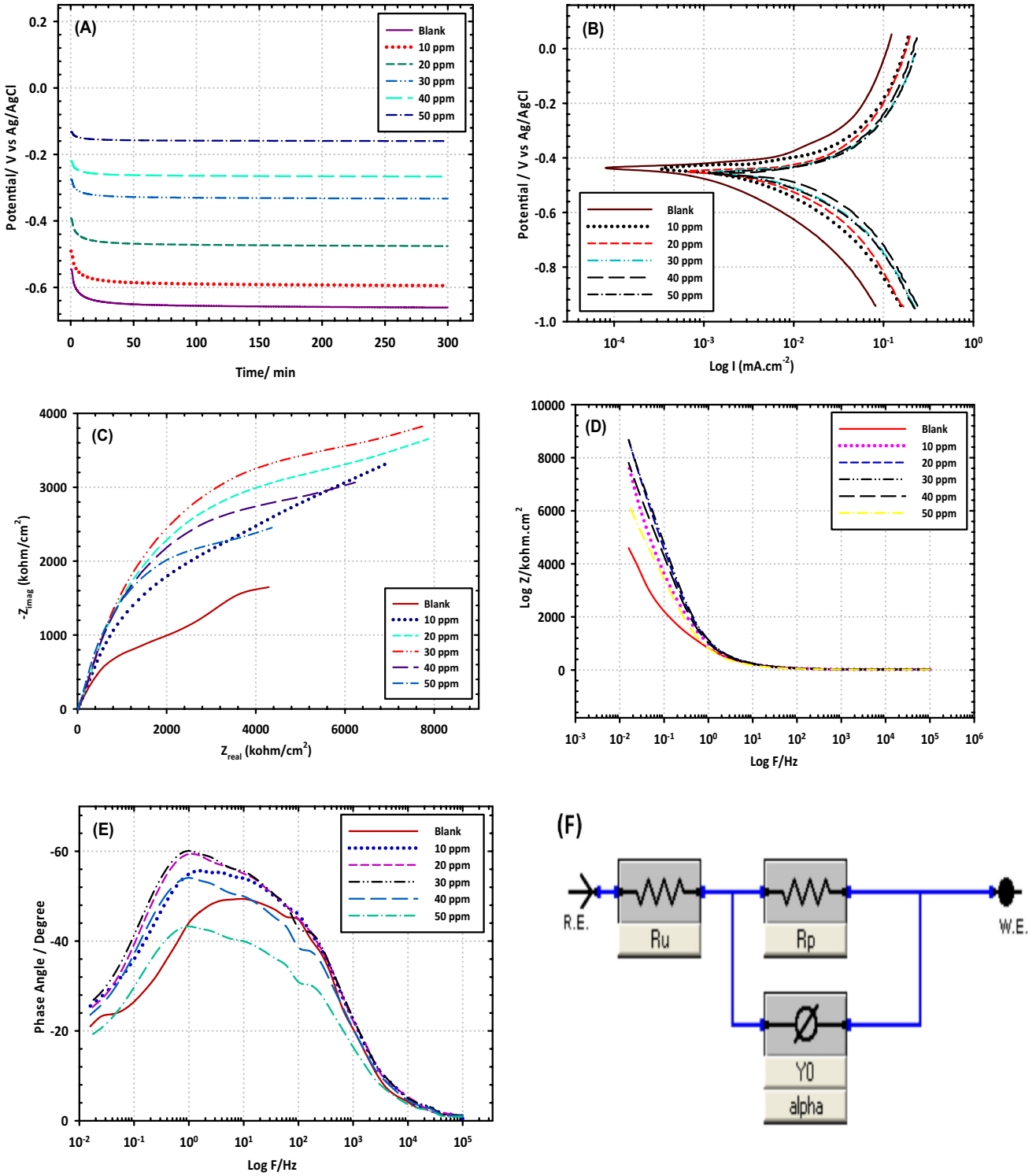

Fig. 1 Electrochemical techniques for carbon steel in the absence and the presence of 1,3-dibutyl thiourea **A** OCP Plots, **B** Potentiodynamic polarization plots, **C** EIS Nyquist Plots, **D** EIS Bode plots, **E** EIS Phase Angle Plots, **F** EIS Equivalent circuit

ring is linked to the damper layer's load transfer resistance. According to Fig. 1C, the capacitance rings get tighter as the concentration of inhibitor increases, owing to the buildup of receptors at the active sites. The treatment will aid in the protection of the metal against hostile attack, intensifying the conflict between the chloride ions and the metal surface. The log|Z|-log f map is an oblique line in the medium

Table 1 Parameters of polarization plots corresponding to the inhibiting effect of various loads of 1,3-dibutyl thiourea as a corrosion inhibitor for carbon steel in 3.5% NaCl

Conc. (ppm)	E (mV)	i_{corr} (μA cm^{-2})	B_a (mV)	B_c (mV)	CR (μm/Y)	θ	IF $_{CR}$%
3.5% NaCl	− 561	0.029	110	− 106	264	–	–
10	− 572	0.015	129	− 115	57	0.79	68.7
20	− 581	0.010	178	− 124	61	0.80	69.5
30	− 598	0.008	182	− 129	44	0.81	75.8
40	− 612	0.006	199	− 132	31	0.83	78.9
50	− 261	0.004	244	− 134	20	0.86	84.6

frequency spectrum that indicates the device has a capacitive nature (see Fig. 1D).

Table 2 describes the fitting parameters found using the matching equivalent circuits. Table 2 shows that there were minor improvements over R_s. It was discovered that the scale is equivalent to the constant value of the damper's electrical insulation, demonstrating the noticeable buildup of the surface retarder [41]. Figure 1E illustrates the computation of impedance and mounting defect for five alternative drilling solutions, as shown in Fig. 1F, except for phases, where the transition results are only in the 10% zone. Because virtually all spontaneous system faults are to be expected, the inquiry results and the proper outcome must be completely consistent.

3.2 (SEM) & (EDX)

SEM images were obtained to examine the development of steel substrates with the presence and absence of DBTU to describe the metallic surface and learn about the inhibitor's protective mechanism. Figure 2A shows an SEM micrograph of an untreated model as a reference sample for comparing treated samples. The metal surface contains high quantities of corrosive elements. An SEM picture of a carbon steel surface exposed to 3.5% (w/w) NaCl for 7 days with the addition of 0.05 g/L (or 50 ppm) of DBTU is shown in Fig. 2C.

The EDX results in Fig. 3 revealed element (*S*) in the presence of DBTU, demonstrating that the inhibitor forms a protective layer on the electrode's surface. While it was not identified in the absence of DBTU (Fig. 3A), these findings show that the source of the element sulfur is a corrosion inhibitor. Furthermore, as compared to the unconstrained carbon steel alloy surface experiment, the Fe^{2+} peaks are deliberately muted. Because the damper membrane is placed on the surface of the steel, these steel manifestations arise [42].

3.3 Antibacterial Effect of DBTU

Figure 4 depicts bacterial proliferation over time in the absence of DBTU. Bacterial growth is easily visible, as the number of bacteria grows after 24 h with time to achieve a value of 106, i.e., it exceeded one million bacterial cells per ml. To evaluate the inhibitor's capacity to block or prevent bacterial growth, different dosages of DBTU were employed to examine the impact utilized to stop bacterial growth, particularly bacteria suspended in solution. The results revealed that the presence of DBTU influenced bacterial growth, particularly on suspended species, and the effect of different inhibitor loading on microbial growth was investigated.

Figure 4 depicted a consistent reduction in bacterial populations as time passed and varied doses of the inhibitor were

Table 2 Parameters of EIS plots corresponding to the inhibiting effect of various loads of 1,3-dibutyl thiourea as a corrosion inhibitor for carbon steel in 3.5% NaCl

Conc. (ppm)	R_s	CPE ($S.s^n/cm^2$)	n	R_p (Ω cm^2)	C_C (mF/cm^2)	CPE ($S.s^n/cm^2$)	n	R_{ct} (Ω cm^2)	C_{dl} (mF/cm^2)	I.E (%)
3.5% NaCl	8	0.0013	0.61	244	0.97	0.0014	0.74	275	1.451	–
10	12	0.0005	0.78	1096	0.80	0.0080	0.79	1120	1.040	30.6
20	14	0.0005	0.81	2409	0.74	0.0006	0.86	2304	0.815	41.5
30	16	0.0001	0.82	3416	0.61	0.0004	0.89	2456	0.653	52.4
40	19	0.0003	0.84	4026	0.50	0.0002	0.91	2832	0.321	67.6
50	21	0.0003	0.86	5336	0.39	0.00009	0.92	3221	0.168	79.5

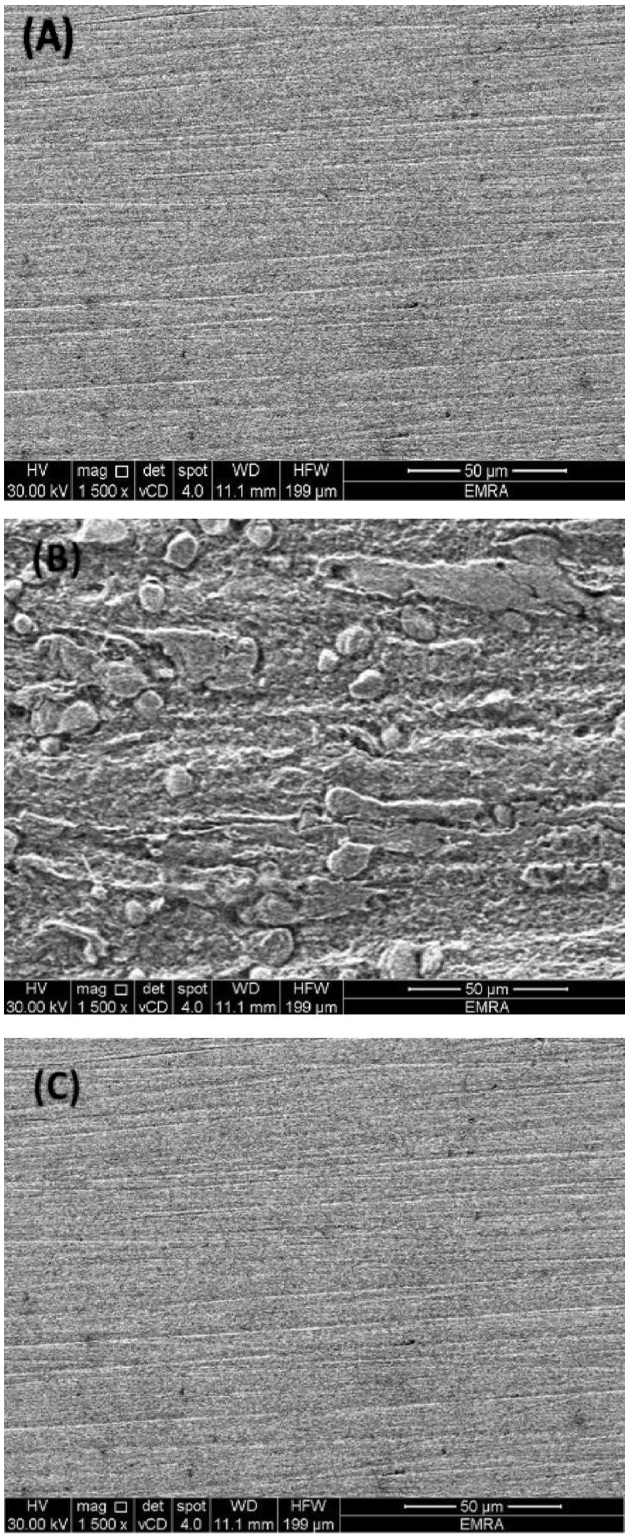

Fig. 2 SEM micrograph of **A** Polished sample, **B** Blank sample, **C** Treated sample with 50 ppm 1,3-dibutyl thiourea

used. After 1 h of inoculation, only 100 colonies/ml was estimated at 100 ppm, and this result is deemed extremely satisfactory in terms of attaining full inhibition after 3 h [43].

3.4 Quantum Chemical Calculations of DBTU

By adjusting bond angles, bilateral angles of surfaces, and bond lengths, the geometric and electronic compositions of DBTU are examined. The optimum and calculated structure with the least amount of energy is depicted in Fig. 5 [44]. As mentioned in Table 3 for DBTU, the geometry of the DBTU is displayed in Fig. 5A, B. The conversion of chemical activity of collaboration between HOMO and LUMO plane representations [45, 46].

The capacity of a molecule to distribute electrons to suitable receptors through empty molecular orbitals is determined by E_{HOMO}. The inhibitor's E_{LUMO} determines its capacity to take electrons, and the inhibitor's established E_{HOMO} values, the ease with which electrons were transported to the d orbital, and the vacant metal surface improved the inhibitor's efficacy (Fig. 5C, D). Minor is the E value, which reflects the increased likelihood that the chemical has inhibitory action. Table 4 shows that the (*E*) gap has a higher value than the (*D*), the basic energy illusion affecting the practical electric field, as it is removed for particle circulation and defense [47].

The stator component has a big energy hole, whereas the permeable component has a tiny power hole. Because they can merely propose electrons to a receiver, permissive parts are more of a complimentary response than stationary parts. Absorption seeks to transmit the most minor electrons, and it might occur in the molecule fraction [48].

3.5 Molecular Docking Study of DBTU

Computer modeling is one approach for determining molecular structure, and molecular fusion is an important tool in the creation of computer medicines. The goal of this molecular fusion was to establish the best possible match with the comparative alignment of the protein and the chemical under study. The DBTU ligand was tested with the protein to determine the compound's capacity to interact with the protein and have a biological impact on microorganisms. As shown in Table 5 and Fig. 6A, B, the fusion study revealed a positive connection between DBTU and protein molecules. The curves of a two-dimensional graph are depicted in Fig. 6D [49].

This link might lead to DBTU energy interactions with apoptosis in bacterial cells. Bond energies are the most often

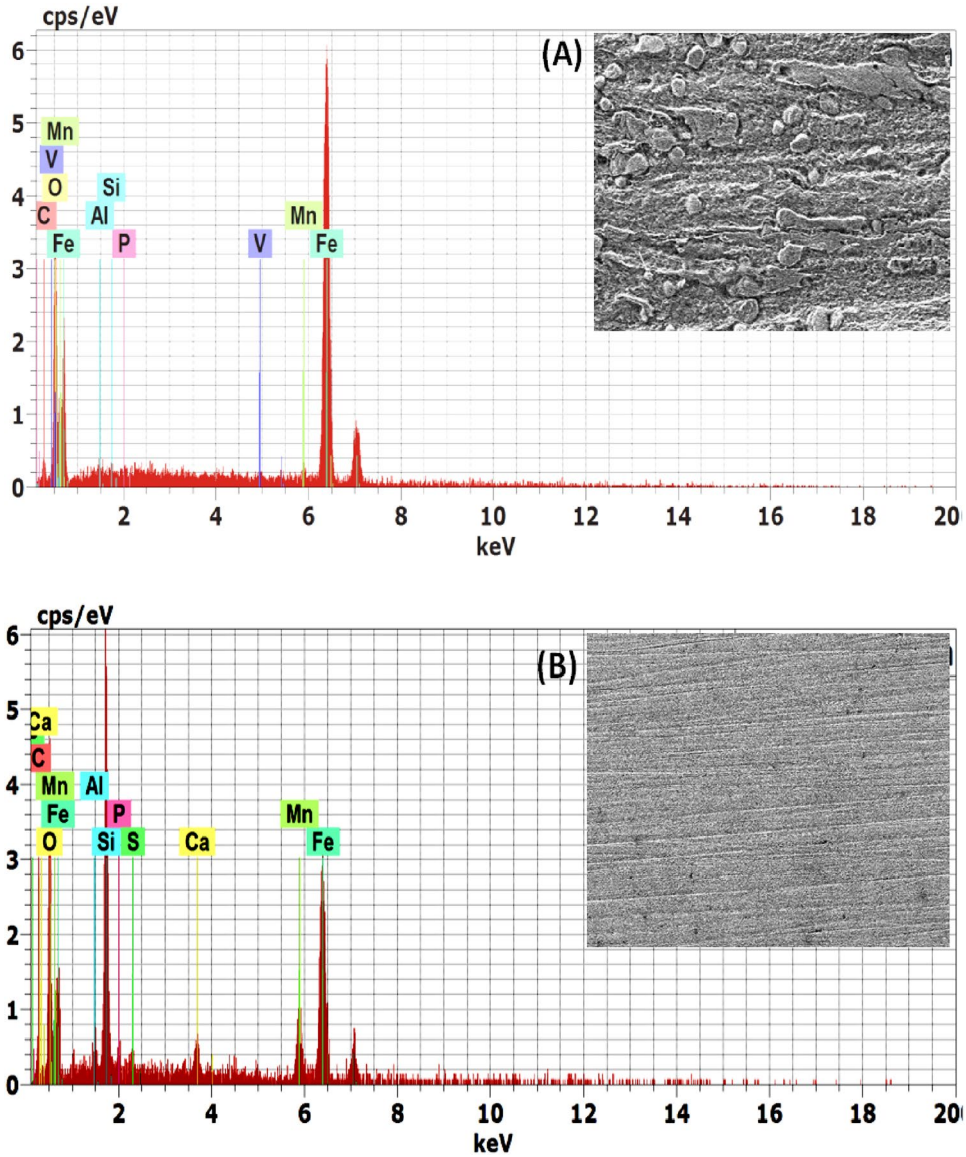

Fig. 3 EDS of **A** Blank and **B** Treated sample with 50 ppm 1,3-dibutyl thiourea

used method for measuring chemical binding affinity. The study discovered that this molecule, DBTU, has a binding capacity of 3.55 kcal/mol and does this using H bonds, static electricity, and van der Waals interactions. This chemical may limit the bacterial growth of microorganisms, making it an efficient bacterial growth inhibitor.

3.6 Mechanism of Microbial Corrosion

The cathodic depolarization theory, also known as the classical theory, was one of the first MIC mechanisms proposed to explain the unusually high rate of corrosion failure seen on subterranean cast iron pipes. When dealing with sulfate-reducing bacteria (SRB) in an anaerobic environment, hydrogen ions are more likely to serve as the cathode's ultimate electron acceptor than when dealing with other bacteria. As a result, the polarized metal surface would be adsorbing the reduced hydrogen concentration. According to previous research, SRB was responsible for depolarizing this cathode by recombination of the atomic hydrogen gas that had been adsorbed onto the cathode via the consumption of cathodic hydrogen by the enzyme hydrogenase [50].

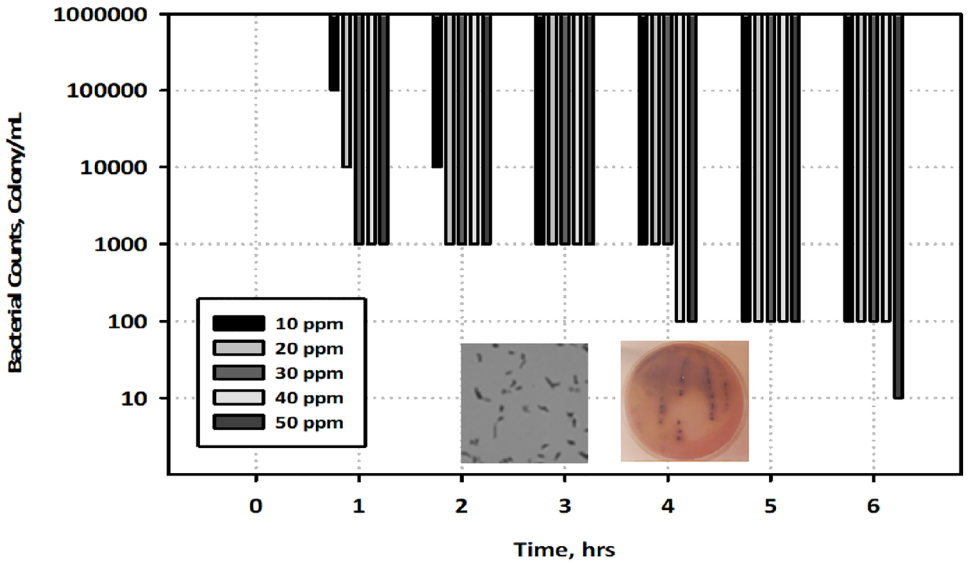

Fig. 4 Microbial corrosion results of 1,3-dibutyl thiourea

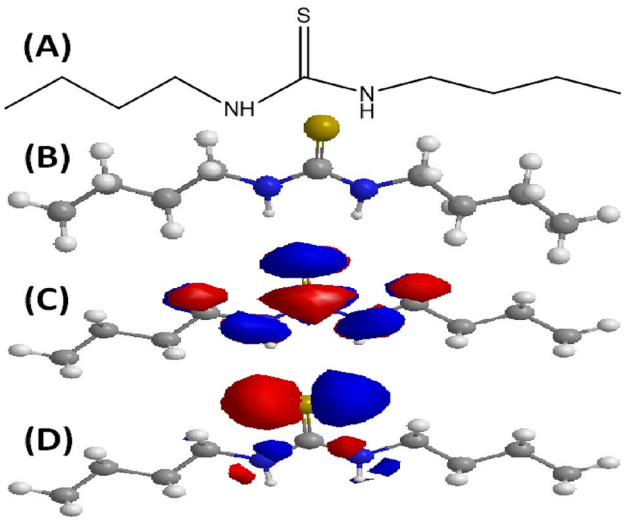

Fig. 5 The optimized formula of 1,3-dibutylthiourea **A** Molecular structure, **B** LUMO (E_{LUMO} = − 6.947 eV (excited state), **C** HOMO (E_{HOMO} = − 8.946 eV (ground state), **D** HOMO and LUMO skeleton

The identification of biocorrosion pathways has been accomplished via the utilization of numerous physiological processes carried out by diverse microorganism types. Because of the large variety of conceivable mechanisms, we are unable to predict a single coherent thought that will bring all these processes together. It has been shown that bacteria may affect the chemical environment around metal surfaces, leading metals to corrode more rapidly than they would otherwise. These modifications are dictated by the properties of the corroding metal as well as the microbial community structure of the biofilm [51].

This is based on the findings of the study, which concluded that identifying microbiological causes of technological equipment failures requires an individual approach to each case and that determining the destructive role of microorganisms present in the surrounding medium can only be determined by analyzing and stimulating the corrosion parameters observed in practice. As a result, the notion that there are multiple mechanisms of MIC rather than a single mechanism is widely accepted in the literature [52].

Table 3 Corresponding bond lengths and bond angles of 1,3-dibutyl thiourea

Bond length (Å)		Bond angel (°)			
C(7)–H(20)	1.113	H(20)–C(7)–H(19)	109.52	H(14)–N(3)–C(2)	120
C(7)–H(19)	1.113	H(20)–C(7)–H(18)	109.462	C(4)–N(3)–C(2)	120
C(7)–H(18)	1.113	H(20)–C(7)–C(6)	109.462	H(13)–C(2)–H(12)	109.52
C(6)–H(17)	1.113	H(19)–C(7)–H(18)	109.442	H(13)–C(2)–N(3)	109.462
C(6)–H(16)	1.113	H(19)–C(7)–C(6)	109.442	H(13)–C(2)–C(1)	109.462
N(5)–H(15)	1.012	H(18)–C(7)–C(6)	109.5	H(12)–C(2)–N(3)	109.442
N(3)–H(14)	1.012	H(17)–C(6)–H(16)	109.52	H(12)–C(2)–C(1)	109.442
C(2)–H(13)	1.113	H(17)–C(6)–C(7)	109.462	N(3)–C(2)–C(1)	109.5
C(2)–H(12)	1.113	H(17)–C(6)–N(5)	109.462	H(11)–C(1)–H(10)	109.52
C(1)–H(11)	1.113	H(16)–C(6)–C(7)	109.442	H(11)–C(1)–H(9)	109.462
C(1)–H(10)	1.113	H(16)–C(6)–N(5)	109.442	H(11)–C(1)–C(2)	109.462
C(1)–H(9)	1.113	C(7)–C(6)–N(5)	109.5	H(10)–C(1)-H(9)	109.442
C(4)–S(8)	1.576	H(15)–N(5)–C(6)	120	H(10)–C(1)–C(2)	109.442
C(6)–C(7)	1.523	H(15)–N(5)–C(4)	120	H(9)–C(1)–C(2)	109.5
N(5)–C(6)	1.45	C(6)–N(5)–C(4)	120	S(8)–C(4)–N(3)	120
C(4)–N(5)	1.369	S(8)–C(4)–N(5)	120	N(5)–C(4)–N(3)	120
N(3)–C(4)	1.369	H(14)–N(3)–C(4)	120		
C(2)–N(3)	1.45				
C(1)–C(2)	1.523				

Table 4 Chemical parameters corresponding to 1,3-dibutyl thiourea result from the calculated quantum obtained from DFT calculations

E_{HUMO}	E_{LUMO}	ΔE	X	η	σ	P_i	S	Ω	ΔN_{max}
− 8.946	− 6.947	1.999	0.9995	7.9465	0.125842	− 0.9995	0.062921	3.969278	0.125779

Table 5 Corresponding energy values were obtained in 1,3-dibutyl thiourea docking measurements with corona 5epw receptor

Est. free energy of binding (kcal/mol)	Est. inhibition Constant, Ki (m/M)	vdW + H-bond + resolve Energy (kcal/mol)	Electrostatic energy (kcal/mol)	Total inter-molec. energy (kcal/mol)
− 3.55	2.48	− 5.88	− 0.01	− 5.89

Simply put, the MIC reported here is due to redox reactions of metals facilitated by microbial ecology because of linked biological and abiotic electron-transfer processes. Measuring the MIC's mechanism is critical because it shows how microbial reactions affect corrosion and, based on that, identifies the products of those reactions on the surfaces of corroding metals using proper analytical methods. As a result, the presence of these compounds may be utilized as evidence to support the particular mechanism of MIC. To understand microorganism-induced corrosion, it is important

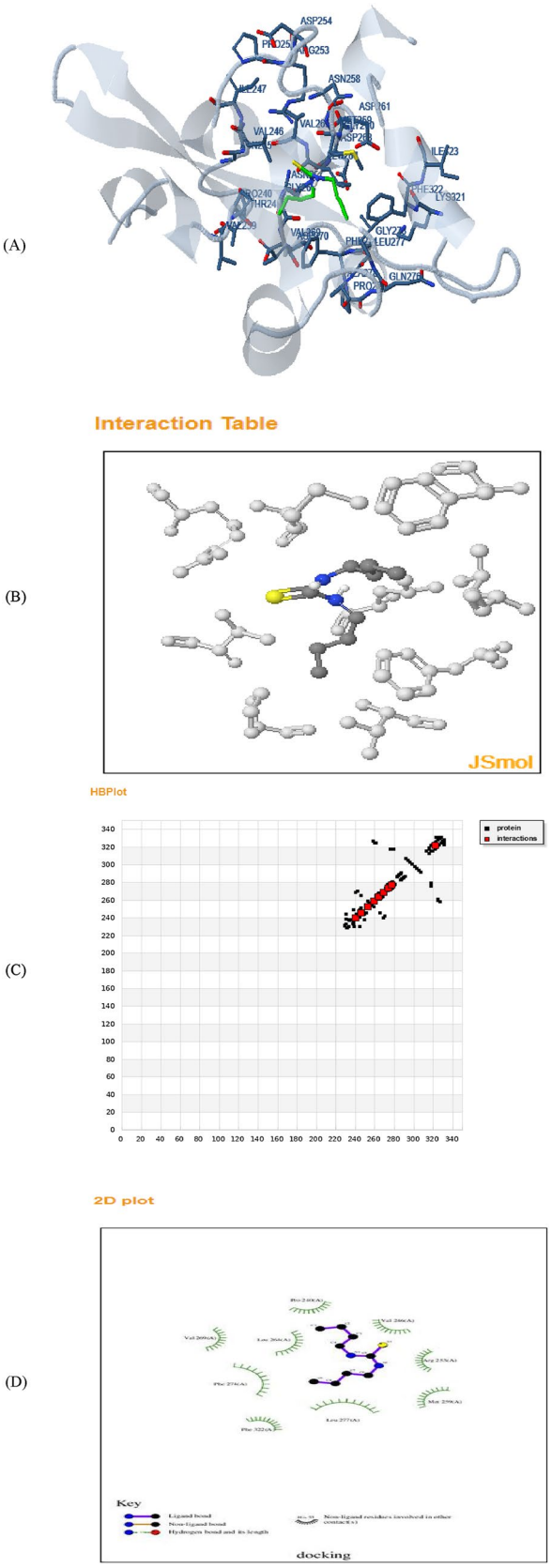

Fig. 6 The quantum aspects of 1,3-dibutyl thiourea **A** Green, **B** Blue ▶ with microbial protein receptor, **C** HB plot of interaction 1,3-dibutyl thiourea with microbial protein receptor, **D** 2D plot of interaction between 1,3-dibutyl thiourea with a microbial protein receptor

to understand the following categories. There is a direct impact on the anodic and cathodic reaction speeds with the first one. The second one focuses on biofilms, which allow for the development of diverse aeration cells in the environment. Because of the acid's creation, there are corrosive media in the third category. The last one is concerned with the impact of metabolic byproducts on the resistance of films erupting from metal surfaces [53].

4 Conclusion

As proven in this article, the DBTU component was investigated as an ecologically safe corrosion inhibitor. In a brine medium containing 3.5 w/w NaCl, this chemical, DBTU, was discovered to be a significant inhibitor for carbon steels. Starting with various dosages, 50 ppm of DBTU demonstrated average inhibitory effectiveness of 95.36%. With a larger temperature range, the affinity for DBTU with the carbon steel surface was strong. Langmuir was discovered to be susceptible to a thermometer by investigating the adsorption of DBTU on carbon steel surfaces. Whereas the thermodynamic adsorption characteristics show that the mechanism of action of carbon steel breakdown is endothermic and that DBTU adsorption can occur via both decomposition and chemical absorption. SEM data from surface assessment research revealed that adding DBTU inhibitors into the aggressive medium reduced the degradation of the surface of carbon steel at 3.5 w/w NaCl throughout treatment. This molecule has also been investigated for its ability to prevent bacterial growth and has demonstrated significant efficacy in decreasing bacterial growth, making it a dual-action compound as it is utilized as an inhibitor of microbial corrosion and erosion. MIC is thought to have multiple mechanisms rather than a single mechanism, according to researchers, who have discovered that detecting MIC in technological equipment failures requires a different approach for each type of failure and that the only way to determine whether microorganisms in the surrounding medium are causing damage is to analyze and simulate corrosion parameters found in the environment, has been discovered.

Funding Not applicable.

Data Availability Data will be available on reasonable request.

Declarations

Conflict of interest The authors declare that there is no conflict of interest.

References

1. Venkata Muralidhar K (2019) (Tata Consultancy Services Limited) Vinay Jain (Tata Consultancy Services Limited) Beena Rai Tata Thiourea Derivatives as Steel Corrosion Inhibitors: Density Functional Theory and Experimental Studies, CORROSION, 24–28 March, Nashville, Tennessee, USA
2. El-Shamy AM (2020) A review on: biocidal activity of some chemical structures and their role in mitigation of microbial corrosion. Egypt J Chem 63(12):5251–5267. https://doi.org/10.21608/ejchem.2020.32160.2683
3. Vinutha MR, Venkatesha TV (2016) Review on mechanistic action of inhibitors on steel corrosion in acidic medi. Port Electrochim Acta 34(3):157–184
4. Luo X, Ci C, Li J, Lin K, Du S, Zhang H, Li X, Cheng YF, Zang J, Liu Y (2019) 4-aminoazobenzene modified natural glucomannan as a green eco-friendly inhibitor for the mild steel in 0.5 M HCl solution. Corros Sci 151:132–142
5. El-Shamy AM, Abdelfattah I, Elshafey OI, Shehata MF (2018) Potential removal of organic loads from petroleum wastewater and its effect on the corrosion behavior of municipal networks. J Environ Manag 219:325–331. https://doi.org/10.1016/j.jenvman.2018.04.074
6. Gholamhosseinzadeh MR, Aghaie H, Zandi MS, Giahi M (2019) Rosuvastatin drug as a green and effctive inhibitor for corrosion of mild steel in HCl and H_2SO_4 solutions. J Mater Res Technol 8:5314–5324
7. Alcántara J, Chico B, Simancas J, Díaz I, de la Fuente D, Morcillo M (2016) An attempt to classify the morphologies presented by different rust phases formed during the exposure of carbon steel to marine atmospheres. Mater Charact 118:65–78
8. Dhaiveegan P, Elangovan N, Nishimura T, Rajendran N (2016) Weathering steel in industrial-marine-urban environment: field study. Mater Trans 57:148–155
9. El-Shamy AM, Shehata MF, Metwally HIM, Melegy A (2018) Corrosion and corrosion inhibition of steel pipelines in montmorillonitic soil filling material. SILICON 10(6):2809–2815. https://doi.org/10.1007/s12633-018-9821-4
10. Saber TMH, El Din TAMK, El Din AM (1992) Dibutyl thiourea as corrosion inhibitor for acid washing of multistage flash distillation plant. Br Corros J 27(2):139–143
11. Tsoeunyane MG, Makhatha ME, Arotiba OA (2019) Corrosion inhibition of mild steel by poly(butylene succinate)-l-histidine extended with 1,6-diisocynatohexane polymer composite in 1 M HCl. Int J Corros 2019:1–12
12. Garg N, Aeron A (2014) Microbes in process. NOVA Science Publishers. Chapter 14, Control of corrosion caused by sulfate-reducing bacteria, pp 337–362
13. Abdallah M, Al-Gorair AS, Fawzy A, Hawsawi H, AbdelHameed RS (2021) Enhancement of adsorption and anticorrosion performance of two polymeric compounds for the corrosion of SABIC carbon steel in hydrochloric acid. J Adhes Sci Technol. https://doi.org/10.1080/01694243.2021.1907041
14. Alfakeera M, Abdallah M, Reda S, Hameed A (2020) Propoxylated fatty esters as safe inhibitors for corrosion of zinc in hydrochloric acid. Prot Met Phys Chem Surf 56(1):225–232. https://doi.org/10.1134/S2070205120010025
15. El-Shamy AM, Soror TY, El-Dahan HA, Ghazy EA, Eweas AF (2009) Microbial corrosion inhibition of mild steel in salty water environment. Mater Chem Phys 114(1):156–159. https://doi.org/10.1016/j.matchemphys.2008.09.003
16. Hameed A, Ismail EA, Al-Shafey HI, Abbas MA (2020) Expired indomethacin drugs as corrosion inhibitors for carbon steel in 1.0 M hydrochloric acid corrosive medium. J Bio- Tribo-Corros 6:114. https://doi.org/10.1007/s40735-020-00403-5
17. Abdel Hameed RS (2019) Schiff' bases as corrosion inhibitor for aluminum alloy in hydrochloric acid medium. Tenside Surfactants Deterg 56(3):209–215
18. El-Shamy AM, Zohdy KM, El-Dahan HA (2016) Control of corrosion and microbial corrosion of steel pipelines in salty environment by polyacrylamide. Ind Chem 2016(2):2. https://doi.org/10.4172/2469-9764.1000120
19. El-Shamy AM, ZakariaAbbas KMA, ElAbedin SZ (2015) Antibacterial and anti-corrosion effects of the ionic liquid 1-butyl-1-methylpyrrolidinium trifluoromethyl sulfonate. J Mol Liq 211:363–369. https://doi.org/10.1016/j.molliq.2015.07.028
20. Abdel Hameed RS (2018) Cationic surfactant- Zn^{+2} system as mixed corrosion inhibitors for carbon steel in sodium chloride corrosive medium. Port Electrochim Acta 36(4):271–283
21. Abdel Hameed RS, Al-bonayan AM (2021) Recycling of some water-soluble drugs for corrosion inhibition of steel materials: analytical and electrochemical measurements. J Optoelectron Biomed Mater 13(2):45–55
22. Kartsonakis IA, Stamatogianni P, Karaxi EK, Charitidis CA (2019) Comparative study on the corrosion inhibitive effect of 2-mecraptobenzothiazole and Na_2HPO_4 on industrial conveying API 5L X42 pipeline steel. Appl Sci 10:290
23. El-Shamy AM, Shehata MF, Gaballah ST, Elhefny EA (2015) Synthesis and evaluation of ethyl (4-(N-(Thiazol-2-Yl) sulfamoyl), phenyl) carbamate (TSPC) as a corrosion inhibitor for mild steel in 0.1 M HCl. J Adv Chem 11(2):3441–3451
24. Khan G, Basirun WJ, Kazi SN, Ahmed P, Magaji L, Ahmed SM, Khan GM, Rehman MA, Badry A (2017) Electrochemical investigation on the corrosion inhibition of mild steel by Quinazoline Schi_ base compounds in hydrochloric acid solution. J Colloid Interface Sci 502:134–145
25. Ismail AIM, El-Shamy AM (2009) Engineering behavior of soil materials on the corrosion of mild steel. Appl Clay Sci 42:356–362. https://doi.org/10.1016/j.clay.2008.03.003
26. Jafari H, Akbarzade K, Danaee I (2019) Corrosion inhibition of carbon steel immersed in a 1 M HCl solution using benzothiazole derivatives. Arab J Chem 12:1387–1394
27. Abdel-Karim AM, El-Shamy AM (2022) A review on green corrosion inhibitors for protection of archeological metal artifacts. J Bio- Tribo-Corros 8:35. https://doi.org/10.1007/s40735-022-00636-6
28. Mohamed AA, Zakaria K, El-Shamy AM, El Abedin SZ (2019) Utilization of 1-butylpyrrolidinium chloride ionic liquid as an eco-friendly corrosion inhibitor and biocide for oilfield equipment: combined weight loss, electrochemical and SEM studies. Phys Chem 235(4):377–406. https://doi.org/10.1515/zpch-2019-1517
29. Kartsonakis IA, Charitidis CA (2020) Corrosion protection evaluation of mild steel: the role of hybrid materials loaded with inhibitors. Appl Sci 10:6594. https://doi.org/10.3390/app10186594
30. Reda Y, Yehia HM, El-Shamy AM (2022) Microstructural and mechanical properties of Al-Zn alloy 7075 during RRA and triple aging. Egypt J Pet 31:9–13. https://doi.org/10.1016/j.ejpe.2021.12.001

31. El-Shamy AM, El-Hadek MA, Nassef AE, El-Bindary RA (2020) Optimization of the influencing variables on the corrosion property of steel alloy 4130 in 3.5 wt% NaCl solution. J Chem 2020:9212491. https://doi.org/10.1155/2020/9212491
32. Abdallah M, Hawsawi H, Al-Gorair AS, Alotaibi MT, Al-Juaid SS, Abdel Hameed RS (2022) Appraisal of adsorption and inhibition effect of expired micardis drug on aluminum corrosion in hydrochloric acid solution. Int J Electrochem Sci 17:220462. https://doi.org/10.20964/2022.04.61
33. Vinothkumar K, Sethuraman MG (2018) Corrosion inhibition ability of electropolymerised composite film of 2-amino-5-mercapto-1,3,4-thiadiazole/TiO_2 deposited over the copper electrode in neutral medium. Mater Today Commun 14:27–39
34. Zohdy KM, El-Shamy AM, Kalmouch A, Gad EAM (2019) The corrosion inhibition of (2Z,2′ Z)-4,4′-(1,2-phenylene bis (azanediyl)) bis (4-oxobut-2-enoic acid) for carbon steel in acidic media using DFT. Egypt J Pet 28(4):355–359. https://doi.org/10.1016/j.ejpe.2019.07.001
35. Dwivedi D, Lepková K, Becker T (2017) Carbon steel corrosion: a review of key surface properties and characterization methods. RSC Adv 7:4580–4610
36. El-Shamy AM, Abdel Bar MM (2021) Ionic liquid as water soluble and potential inhibitor for corrosion and microbial corrosion for iron artifacts. Egypt J Chem 64(4):1867–1876. https://doi.org/10.21608/ejchem.2021.43786.2887
37. El-Shamy AM, El-Boraey HA, El-Awdan HF (2017) Chemical treatment of petroleum wastewater and its effect on the corrosion behavior of steel pipelines in sewage networks. J Chem Eng Process Technol 2017:1–8. https://doi.org/10.4172/2157-7048.1000324
38. Shehata M, El-Shafey S, Ammar NA, El-Shamy AM (2019) Reduction of Cu^{2+} and Ni^{2+} ions from wastewater using mesoporous adsorbent: effect of treated wastewater on corrosion behavior of steel pipelines. Egypt J Chem 62:1587–1602. https://doi.org/10.21608/ejchem.2019.7967.1627
39. Reda Y, El-Shamy AM, Zohdy KM, Eessaa AK (2020) Instrument of chloride ions on the pitting corrosion of electroplated steel alloy 4130. Ain Shams Eng J 11:191–199. https://doi.org/10.1016/j.asej.2019.09.002
40. Abdallah M, Abdel Hameed RS, Al-Bagawi AH, Shehata HA, Shamroukh AH (2020) Corrosion inhibition and adsorption properties of some heterocyclic derivatives on C- steel surface in HCl. J Bio-tribio Corros 51(6):1–11. https://doi.org/10.1007/s40735-020-00345-y
41. El-Shamy AM, Alkharafi FM, Abdallah RM, Ghayad IM (2010) Electrochemical oxidation of hydrogen sulfide in polluted brines using porous graphite electrodes under geothermal conditions. Chem Sci J 2010:1–12
42. Reda Y, Zohdy KM, Eessaa AK, El-Shamy AM (2020) Effect of plating materials on the corrosion properties of steel alloy 4130. Egypt J Chem 63:579–597. https://doi.org/10.21608/ejchem.2019.11023.1706
43. Anaee RA, Tomi IHR, Abdulmajeed MH, Nangia SA, Kathem MMN (2019) Expired etoricoxib as a corrosion inhibitor for steel in acidic solution. J Mol Liq 279:594–602
44. Mouneir SM, El-Hagrassi AM, El-Shamy AM (2022) A review on the chemical compositions of natural products and their role in setting current trends and future goals. Egypt J Chem 65(5):491–506. https://doi.org/10.21608/ejchem.2021.95577.4486
45. Lukovits I, Kalman E, Zucchi F (2001) Corrosion inhibitors correlation between electronic structure and efficiency. Corrosion 57:3–8
46. Guo W, Umar A, Zhao Q, Alsaiari MA, Al-Hadeethi Y, Wang L, Pei M (2020) Corrosion inhibition of carbon steel by three kinds of expired cephalosporins in 0.1 M H_2SO_4. J Mol Liq 320:114295
47. Megahed MM, Youssif M, El-Shamy AM (2020) Selective formula as a corrosion inhibitor to protect the surfaces of antiquities made of leather-composite brass alloy. Egypt J Chem 63(12):5269–5287. https://doi.org/10.21608/ejchem.2020.41575.2841
48. Zohdy KM, El-Sherif RM, Ramkumar S, El-Shamy AM (2021) Quantum and electrochemical studies of the hydrogen evolution findings in corrosion reactions of mild steel in acidic medium. Upstream Oil Gas Technol 6:100025. https://doi.org/10.1016/j.upstre.2020.100025
49. El-Bindary R, El-Shamy A, Elhadek MA, Nassef A (2021) Statistical analysis of the inhibition of carbon steel corrosion in 3.5 wt% NaCl solution using lawsonia extract. Port-Said Eng Res J 25(1):101–113. https://doi.org/10.21608/pserj.2020.35020.1050
50. Zohdy KM, El-Sherif RM, El-Shamy AM (2021) Corrosion and passivation behaviors of tin in aqueous solutions of different pH. J Bio-Tribo–Corros 7(2):1–7. https://doi.org/10.1007/s40735-021-00515-6
51. Megahed MM, Abdel Bar MM, Abouelez ESM, El-Shamy AM (2021) Polyamide coating as a potential protective layer against corrosion of iron artifacts. Egypt J Chem 64(10):5693–5702. https://doi.org/10.21608/ejchem.2021.70550.3555
52. Reda Y, Abdelbar M, El-Shamy AM (2021) Fortification performance of polyurethane coating in outdoor historical ironworks. Bull Natl Res Cent 45:69. https://doi.org/10.1186/s42269-021-00532-y
53. Abdel-Karim AM, El-Shamy AM, Reda Y (2022) Corrosion and stress corrosion resistance of Al Zn Alloy 7075 by nano-polymeric coatings. J Bio- Tribo-Corros 8:57. https://doi.org/10.1007/s40735-022-00656-2